Studies on Mesomorphic Behaviors of Segmented Azoxy Polyester Containing Polyoxyethylene

JAINE MING HUANG, JEN FENG KUO,* and CHUH YUNG CHEN

Department of Chemical Engineering, National Cheng-Kung University, Tainan, Taiwan 70101, Republic of China

SYNOPSIS

A series of a segmented copolymer, poly(4,4'-dioxy-2,2'-dimethyl-azoxybenzene dodecanedioyl)-*co*-polyoxyethylene 400 (PMABD-*co*-POE) was prepared; the average chain lengths n, of the PMABD studied are 8.1 to 20.6. The thermotropic properties and the mesophase texture of the segmented copolymers were elucidated as functions of n using a differential scanning calorimeter and a polarized optical microscope with a hot stage. The results show that the incorporation of POE with PMABD decreases the intermolecular interaction force and changes the chain flexibility. The nematic droplets obtained near the isotropic temperature all exhibited a twisted bipolar configuration. Also, in the undercooling process, the nematic textures obtained before crystallizing varied with n. The copolymers containing $n \geq 17$, like PMABD, develop a Schlieren texture, whereas those containing $n < 17$ develop a distorted-stripe conformation. A possible mechanism for interpretation of the obtained results has been proposed. © 1995 John Wiley & Sons, Inc.

INTRODUCTION

Since they were first described by Roviello and Sirigu,[1] thermotropic polymeric liquid crystals (PLCs), which are composed of an alternative arrangement of a mesogenic unit and flexible spacer groups in the main chain, have been extensively studied.[2-18] Like the mesogenic unit in PLCs, the flexible spacer also plays an important role in determining not only the thermotropic properties but also the mesomorphic behaviors.[2-13] In consideration of the aspect of using flexible spacers to tailor mesophase and properties of a liquid crystalline (LC) polymer, the structural factors considered usually are the chain length, even/odd effect, chirality, polarizability, a single mesogenic group with two spacers of different length,[2-7] or with a chiral spacer and an ordinary spacer.[8-12]

LC polyesters with the 4,4'-dihydroxyazoxybenzene and/or 4,4'-dihydroxy-2,2'-dimethyl-azoxybenzene moiety in the main chain have been extensively studied by Blumstein et al.[9-13] The polymers containing a methylene spacer show a nematic mesophase and a strong and regular even–odd effect. According to de Gennes,[19] molecular length, intermolecular interactions, and chain rigidity determine the elastic constants: the spray constant K_{11}, the twisting constant K_{22}, and the bending constant K_{33}, and then dominate the microscope texture of nematic droplets (NDs). Thus, the change of chain lengths, or polarity of spacers, may lead to influence the microscope texture of NDs, in addition to those thermotropic properties usually focused on. The present work was to prepare a series of poly(4,4'-dioxy-2,2'-dimethyl-azoxybenzene dodecanedioyl) (PMABD)-*co*-polyoxyethylene 400 (POE). The copolymer possesses characteristics of a segmented structure in which the average chain length of the PMABD segment studied is 8–20. The aim of this work was to study the effects of incorporation of the PMABD segments with a given length of POE on the mesophase texture of the nematic LC phase and the thermotropic properties of PMABD.

EXPERIMENTAL

Materials

Tetraammonium hydrogen sulfate, *m*-cresol, pyridine (from Merck Co.), sodium nitrite, tosyl chloride,

* To whom correspondence should be addressed.

Journal of Applied Polymer Science, Vol. 55, 1217–1229 (1995)
 CCC 0021-8995/95/081217-13

thionyl chloride, sodium hydroxide (from Ferak Co.), dodecanedioic acid (from Sigma Chemical Co.), and poly(ethylene glycol) ($\bar{M}_n$ = 400, from Wako Chemical Co. Japan) were used as received.

Techniques

^{1}H-NMR spectra were recorded on a Bruker AMX 400 from $CDCl_3$ and *d*-acetone solutions. The composition of the segmented copolyester was determined by a Heraeus CHN-O-RAPID elemental analyzer (EA). The intrinsic viscosities of the copolyesters was measured in 1,1,2,2-tetrachloroethane (TCE) at 30°C by a Schott Gerate AVS310 with the type 531 01 capillary viscometer. The phase-transition temperatures of the segmented copolyesters were studied using a DuPont 910 differential scanning calorimeter (DSC) equipped with a liquid nitrogen cooling accessory and a 9900 computer system for data acquisition. The anisotropic textures of copolyesters were examined using an Olympus BH-2 polarizing optical microscopy equipped with a Linkam THMS 600 hot stage and a TMS 91 center processor.

Synthesis

Scheme 1 summarizes the procedures for obtaining 3-methyl-4-nitrosophenol, 4,4′-dihydroxy-2,2′-dimethyl-azoxybenze (DMAB), poly(4,4′-dioxy-2,2′-dimethyl-azoxybenzene-dodecanedioyl) (PMABD), and poly(4,4′-dioxy-2,2′-dimethyl-azoxybenzene-dodecanedioyl-*co*-polyoxyethylene 400) [(PMABD-*co*-POE) polymer].

3-Methyl-4-nitrosophenol

A solution of 22.9 g of *m*-cresol, 9.0 g of sodium hydroxide, and 18.04 g of sodium nitrite in 500 mL of water was cooled to −3°C. To this solution was added with stirring 50 g of sulfuric acid in 140 mL of water at a rate sufficiently slow to maintain the temperature of the reaction mixture at −3 to 0°C. The solution was then stirred at 0°C for an additional 2 h. The brownish precipitate was collected and washed with plenty of water and 30 mL of alcohol, then dried in vacuum at room temperature. The yield was 22 g (76%).

ANAL: Calcd for $C_7H_7NO_2$: C, 61.31%; H, 5.15%; N, 10.20%.
Found: C, 61.19%; H, 5.16%; N, 9.92%.

^{1}H-NMR (*d*-acetone) δ: 2.16(s, 3H, Ar$\underline{CH_3}$); 6.25(d, J = 1.5Hz, 1H, aromatic proton); 6.36(dd, J = 10.2, 2.0Hz, 1H, aromatic proton); 7.77(d, J = 10.2Hz, 1H, aromatic proton); 12.41(s, 1H, Ar$\underline{OH}$).

4,4′-Dihydroxy-2,2′-dimethyl-azoxybenzene

The mesogen 4,4′-dihydroxy-2,2′-dimethyl-azoxybenzene was prepared from 3-methyl-4-nitrosophenol by reductive coupling followed by the two-step synthesis suggested by Leonard and Curry.[20] A mixture of 6.85 g of 3-methyl-4-nitrosophenol and 4.765 g of tosyl chloride in 35 mL of pyridine was stirred at room temperature for 12 h. The solution was then refluxed at 110°C for 20 min, cooled, and acidified with 25% sulfuric acid. The resulting tarry suspension was well extracted with ether. The yellow ethereal extract was sufficiently washed with water. Then, the ether solvent in the extract was distilled off to leave crude products, which was further washed with benzene to remove the byproduct of toluenesulfonic ester and dried. Recrystallization from tetrachloroethane gave a yellow needlelike product with an mp of 184°C, with decomposition. The yield was 2.3 g (35%). The product was identified by EA and ^{1}H-NMR.

Table I The Structure Parameters of Polymers Obtained from ^{1}H-NMR Spectra

Polymer	DMAB/DDAC/POE[a]	α[b]	β[b]	$\gamma = X$[b]	n[b]	$\bar{M}_n$	Wt % of POE
#1	9/10/—	—	19.50	—	19.5	9100	0.0
#2	9/10/1	39.08	43.44	1.11	20.6	20600	2.2
#3	7/8/1	27.95	43.54	1.56	17.0	20900	3.0
#4	5/6/1	20.68	50.62	2.45	14.7	24600	4.0
#5	3/4/1	15.19	51.92	3.42	11.8	25800	5.3
#6	1/2/1	9.41	56.97	6.05	8.1	29600	8.2

[a] Mole ratio of reactants in the feed and DMABs were kept at 0.5 g.
[b] For the definitions of these structure parameters, see the text.

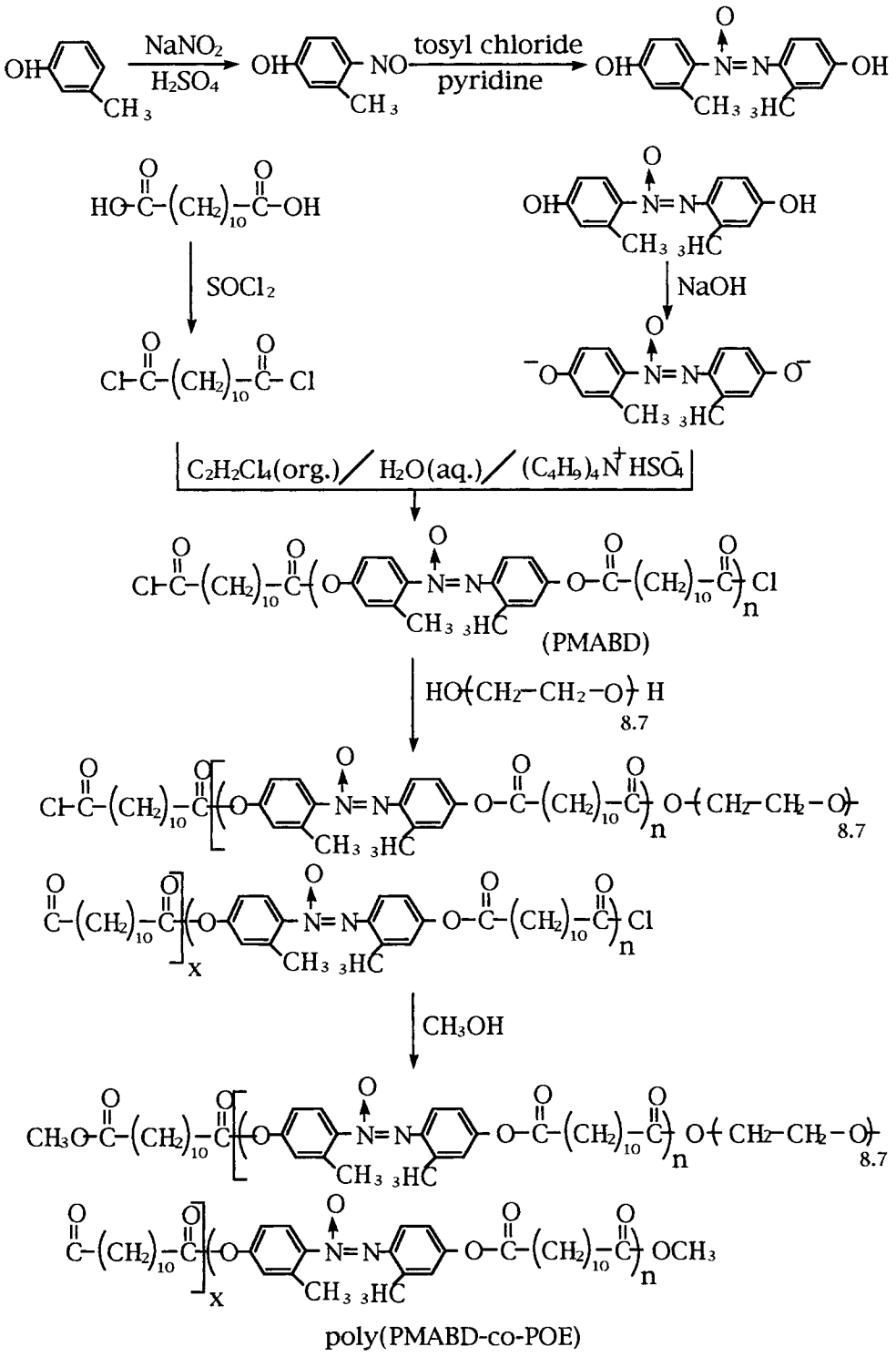

Scheme 1 Procedures for preparation of the main-chain LC polymer, PMABD, and segmented (PMABD-*co*-POE) polymer.

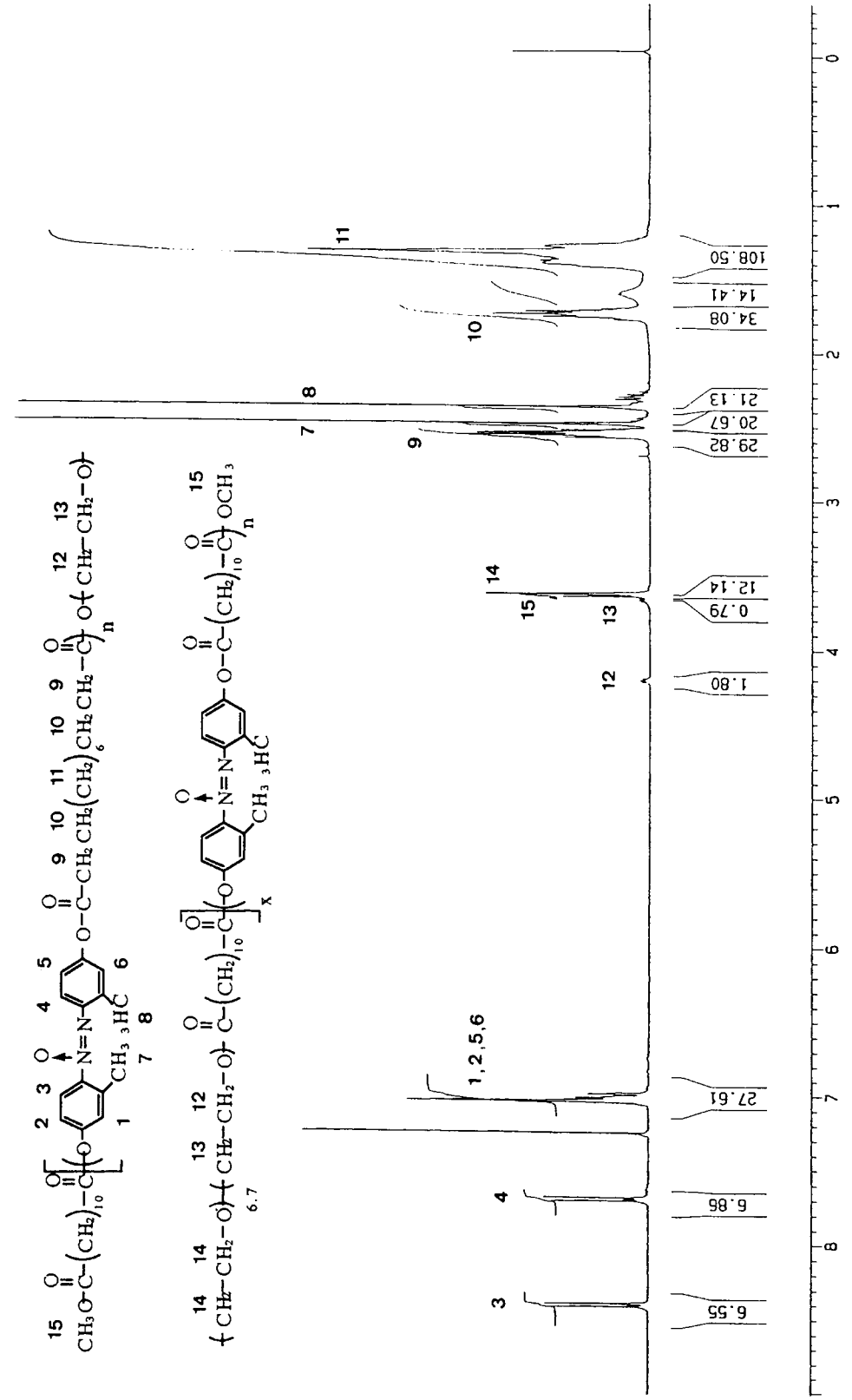

Figure 1 ^{1}H-NMR spectrum of (PMABD-*co*-POE) polymer (#4) in $CDCl_3$.

ANAL: Calcd for $C_{14}H_{14}N_2O_3$: C, 65.10%; H, 5.46%; N, 10.85%.
Found: C, 64.82%; H, 5.47%; N, 10.72%.

^{1}H-NMR (*d*-acetone) δ: 2.34, 2.41(2s, 3H, Ar$\underline{CH_3}$); 6.71–6.81(m, 4H, aromatic protons); 7.59, 8.59(2d, J = 9.2Hz, 1H, aromatic proton); 9.0–9.1(m, 2H, Ar$\underline{OH}$).

Poly(4,4′-dioxy-2,2′-dimethyl-azoxybenzene-dodecanedioyl-*co*-polyoxyethylene 400)

All the copolymers listed in Table I were synthesized by the same procedure, of which sample #4 is an example. The acid chloride was prepared from dodecanedioic acid with thionyl chloride. POE was treated with anhydrous magnesium sulfate ($MgSO_4$) and filtered to remove water completely before use. The polyesterification was carried out by two-step interfacial polycondensation at the water–TCE interface. In a typical reaction, 0.06 g of tetraammonium hydrogen sulfate and 0.5 g of 4,4′-dihidroxy-2,2′-dimethyl-azoxybenzene (DMAB) were dissolved in 5 mL of 1.5*M* sodium hydroxide aqueous solution and was stirred vigorously. Dodecandioic acid chloride (DDAC) (2.326 mmol) was first dissolved in 5 mL of TCE, then rapidly added into the above aqueous solution and the stirring was continued at room temperature until the aqueous solution changed from a dark red color to transparent, i.e., DMAB in the aqueous solution was reacted with DDAC nearly completely, 0.387 mmol of POE in 5 mL of TCE was added, and the solution was continuously stirred at room temperature for an additional 2 h. The product of the copolymer was precipitated by adding an excess of methanol and filtered, then washed with acetone. The copolymer obtained was purified by extraction with methanol in a Soxhlet apparatus for 24 h and dried in vacuum at 60°C. The product was identified by ^{1}H-NMR.

^{1}H-NMR ($CDCl_3$) δ: 2.34, 2.50(2s, 3H, Ar$\underline{CH_3}$); 6.99–7.05(m, 4H, aromatic protons); 7.69, 8.40(2d, J = 8Hz, 1H, aromatic proton); 2.54–2.55, 1.73–1.80(2m, 4H, methylene protons); 1.31–1.43(m, 12H, methylene protons); 4.20(t, J = 4Hz, 4H, 2COO-$\underline{CH_2}CH_2O$); 3.67(t, J = 4Hz, 4H, 2COOCH$_2\underline{CH_2}$O); $\overline{3.65}$(m, 27H, methylene protons); 3.66(s, 6H, $\overline{2OCH_3}$).

Figure 1 illustrates the ^{1}H-NMR spectrum of #4. As indicated by Blumstein et al.,[13] if the last units of PMABD are DMAB, there would appear two small doublet peaks at 8.25 and 8.65 ppm in the spectra, which are due to the 3′- and 3″-protons of the benzyl of the last DMAB. These two peaks are not observed for all the copolymers obtained, which indicates that the (PMABD-*co*-POE) polymers are mostly terminated with methoxylated dodecanedioyl.

Number-average Molecular Weight and Composition of Copolymer Obtained

Following the results of the ^{1}H-NMR spectra, the chemical structure of the segmented copolymer is expressed as follows:

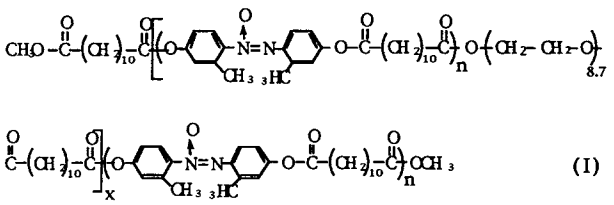

(I)

where **n** denotes the average chain length of the PMABD segment. *X* refers to the average chain length of the repeating unit, which is composed of PMABD and -oxy-polyethyleneoxide-dodecanedioyl-(PEOD).

The mol ratio of DMAB to POE in the copolymer, α, can be determined from the ratio of the total areas of the peaks of the six benzyl protons to the one and one-half of the area of the peak of the methylene protons of terminal oxyethylene units connected di-

Table II Elemental Analysis of Polymers

	Expected (%)			Experimental (%)		
Samples	C	H	N	C	H	N
#1	68.70	7.14	6.00	68.64	7.15	5.68
#2	68.67	7.19	5.92	68.64	7.38	5.98
#3	68.55	7.21	5.84	68.48	7.46	5.74
#4	68.40	7.24	5.76	68.49	7.34	5.64
#5	68.24	7.28	5.65	68.32	7.25	5.78
#6	67.81	7.36	5.39	67.88	7.34	5.53

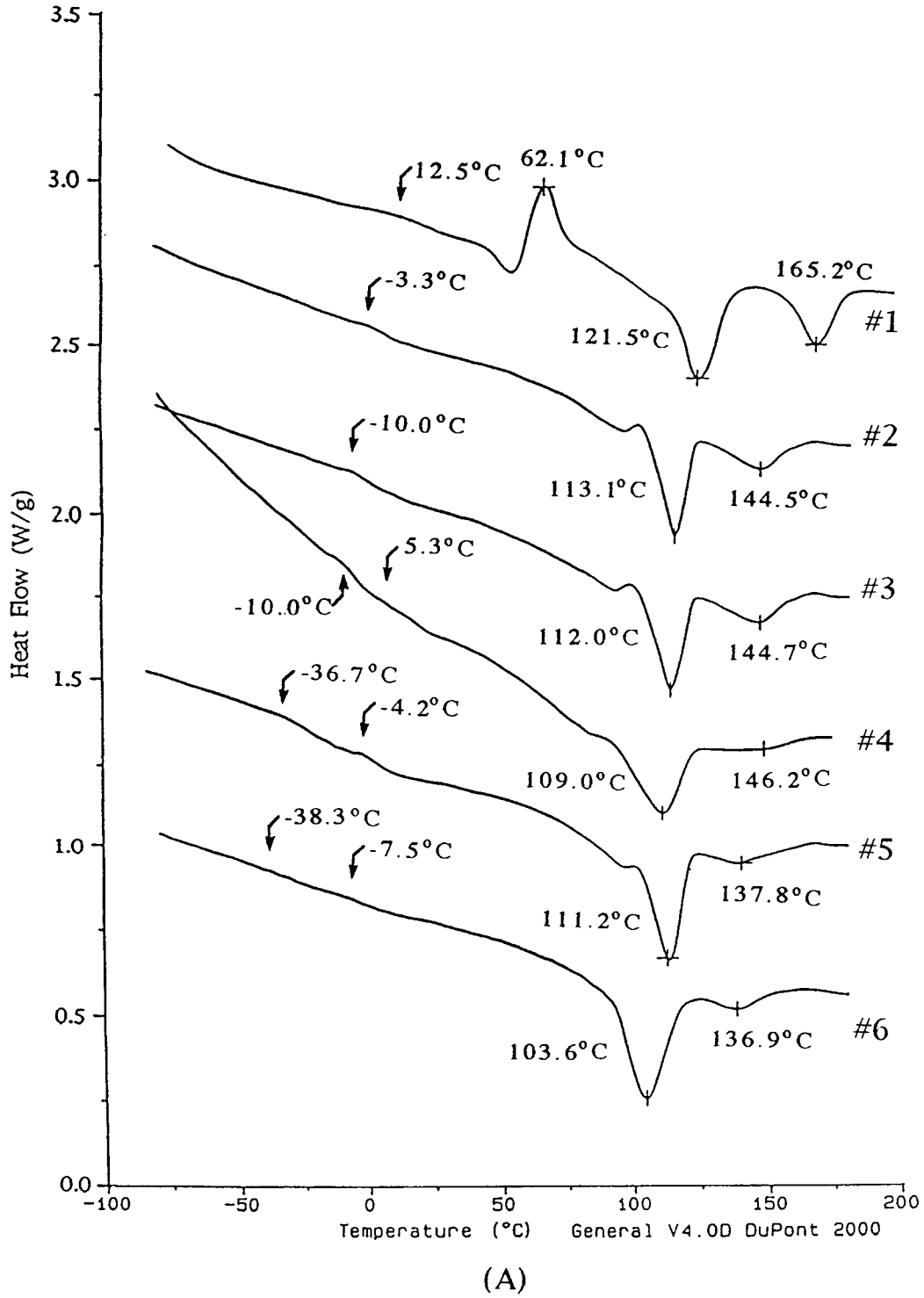

Figure 2 DSC (A) heating and (B) cooling curves of LC polymers; rate: 10°C/min.

rectly to DDA, whereas the average mol of DMAB per mol (PMABD-*co*-POE) polymer, β, was estimated from the ratio of the total areas of the peaks of the six benzyl protons to that of the peak of both the terminal methoxy protons of copolymer. Hence, the ratio β/α $(=\gamma)$ is the average mol of POE per mol of the copolymer. From the structure parameters, β and X, the number-average molecular weight of the copolymer, $\bar{M}_n$, could be estimated using the following equations:

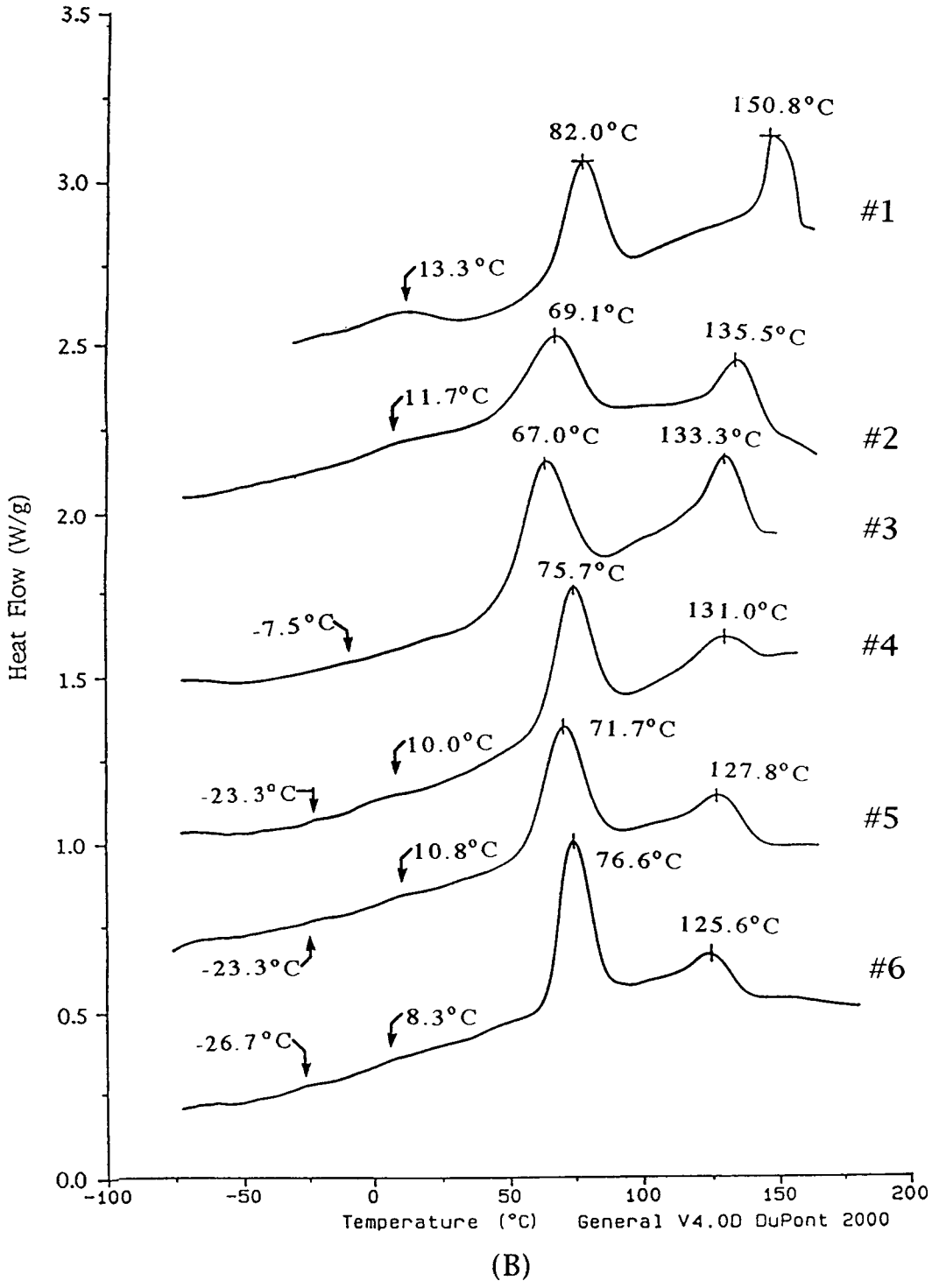

(B)

Figure 2 *(Continued from the previous page)*

$$\bar{M}_n = 452\beta + 594X + 258 \quad (1)$$

$$\mathbf{n} = (\beta - 1)/X \quad (2)$$

where 452 is the molecular weight of repeating unit of PMABD, 594 is the molecular weight of the PEOD, and 258 is that of a dedecanedioyl methoxylate.

The values of α, β, X, $\bar{M}_n$, and weight percent POE of the copolymers obtained are given in Table

Table III The Intrinsic Viscosities and Number-average Molecular Weights of the Polymers

Polymer	$[\eta]$ (dL/g)	$\bar{M}_n$[a] (g/mol)	$\bar{M}_n$[b] (g/mol)
#1	0.47	9,000	9,100
#2	0.88	20,500	20,600
#3	0.90	21,100	20,900
#4	1.04	25,500	24,600
#5	1.05	25,900	25,800
#6	1.18	30,200	29,600

[a] Derived from the Blumstein equation $[\eta]_{TCE}^{30°C} = 4.65 \times 10^{-4} \bar{M}_n^{0.76}$.
[b] By NMR spectroscopy.

I. The $\bar{M}_n$'s of the PMABD-*co*-POE polymer are 2 $\times 10^4$ to 3 $\times 10^4$. Obviously, the smaller the **n** the higher the $\bar{M}_n$ of the copolymer. Table II shows the compositions of nitrogen, carbon, and hydrogen of the copolymers obtained by the elementary analysis (EA). It is found that both the results of EA and ^{1}H-NMR method do not differ more than 5% by weight.

RESULTS AND DISCUSSION

As shown in Table I, the average chain length of PMABD per mol PEOD of the copolymer prepared, n, is 20.6 to 8.1. The number-average molecular weights of the copolymer obtained are 20,600–29,500. As suggested by Blumstein,[9] the transition properties of the melting and mesophase to the isotropic phase of PMABD almost unchange with molecular weight as the average chain length of PMABD is above 10. In the study, except for #6 in which PMABD segments has $n = 8.1$, the others are all above 10. Therefore, in this work, the average chain length of the PMABD segment per mol PEOD is considered to be a main structure factor affecting the thermotropic properties and mesophase texture.

Dilute-solution Properties

The intrinsic viscosities of (PMABD-*co*-POE) polymers, $[\eta]$, were measured in TCE at 30°C using an Ubbelohde-Cannon viscometer. The results are given in Table III. The $[\eta]$'s obtained are all larger than 1 and increase with decreasing n. The Blumstein equation[12] is used for the calculation of $\bar{M}_n$ of the copolymer, i.e.,

$$[\eta]_{TCE}^{30°C} = 4.65 \times 10^{-4} \bar{M}_n^{0.76} \quad (3)$$

Thus, the $\bar{M}_n$'s obtained are in a good agreement with those obtained by the ^{1}H-NMR method. It reveals that in the range of compositions studied the viscosity property of the (PMABD-*co*-POE) polymer in TCE is close to that of pure PMABD.

Thermotropic Properties of the LC Polymers

Figure 2 shows the heating and cooling DSC thermograms for PMABD and the series of (PMABD-*co*-POE) polymers. The thermograms were obtained from the second scans. During both thermal histories, the copolymers studied all appeared to be liquid crystal (LC). Hence, the copolymers show enantiotropic ones. Table IV summarizes the glass transition T_g, the melting T_m, and the isotropic phase transition temperature T_i and the changes of the

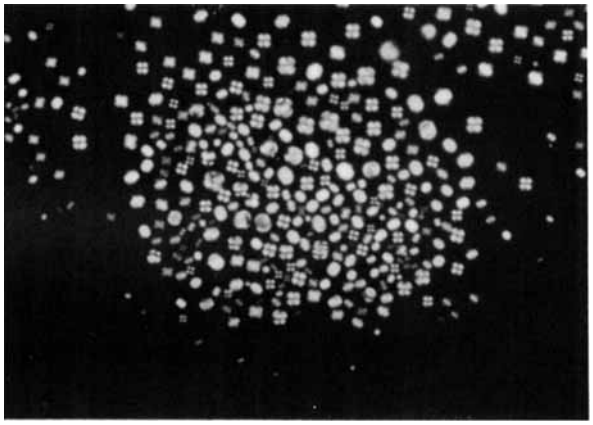

(A)

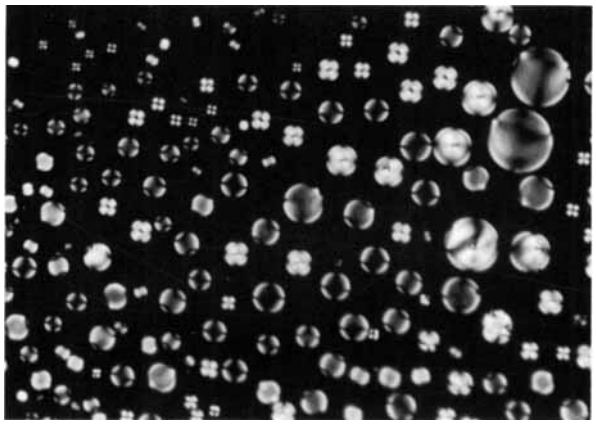

(B)

Figure 3 Polarized optical micrographs (600×) of nematic droplets of PMABD obtained (A) at 132°C for $n = 8$ and (B) at 145°C for $n = 20$.

Table IV Thermal Properties of PMABD and (PMABD-*co*-POE) polymers

Samples	Heating (Cooling)	Transition Temperature (°C) ΔH_{kn} (J/g) (kJ/mru)[a]	ΔS_{kn} (J/gK) (J/Kmur)[a]	ΔH_{ni} (J/g) (kJ/mru)[a]	ΔS_{ni} (J/gK) (J/Kmru)[a]
#1	g13k122n165i	32.76	0.085	18.08	0.041
	(i151n82k-13g)	*(14.81)*	*(38.43)*	*(8.17)*	*(18.5)*
#2	g-3k113n144i	26.05	0.067	6.34	0.015
	(i136n69k12g)	*(11.77)*	*(30.28)*	*(2.87)*	*(6.78)*
#3	g-10k112n145i	26.63	0.069	6.15	0.015
	(i133n67k-8g)	*(12.04)*	*(31.39)*	*(2.78)*	*(6.78)*
#4	g_1-10$g_2$5K109n146i	28.33	0.074	3.74	0.009
	(i131n76k10g_2-23g_1)	*(12.81)*	*(33.45)*	*(1.69)*	*(4.07)*
#5	g_1-37g_2-4k111n138i	27.28	0.071	4.67	0.011
	(il28n72k11g_2-23g_1)	*(12.33)*	*(32.09)*	*(2.11)*	*(4.97)*
#6	g_1-38g_2-8k104n137i	28.92	0.077	3.82	0.009
	(i126n77k8g_2-27g_1)	*(13.07)*	*(34.80)*	*(1.73)*	*(4.07)*

[a] mru = mole of repeating unit:

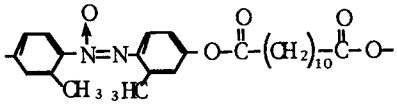

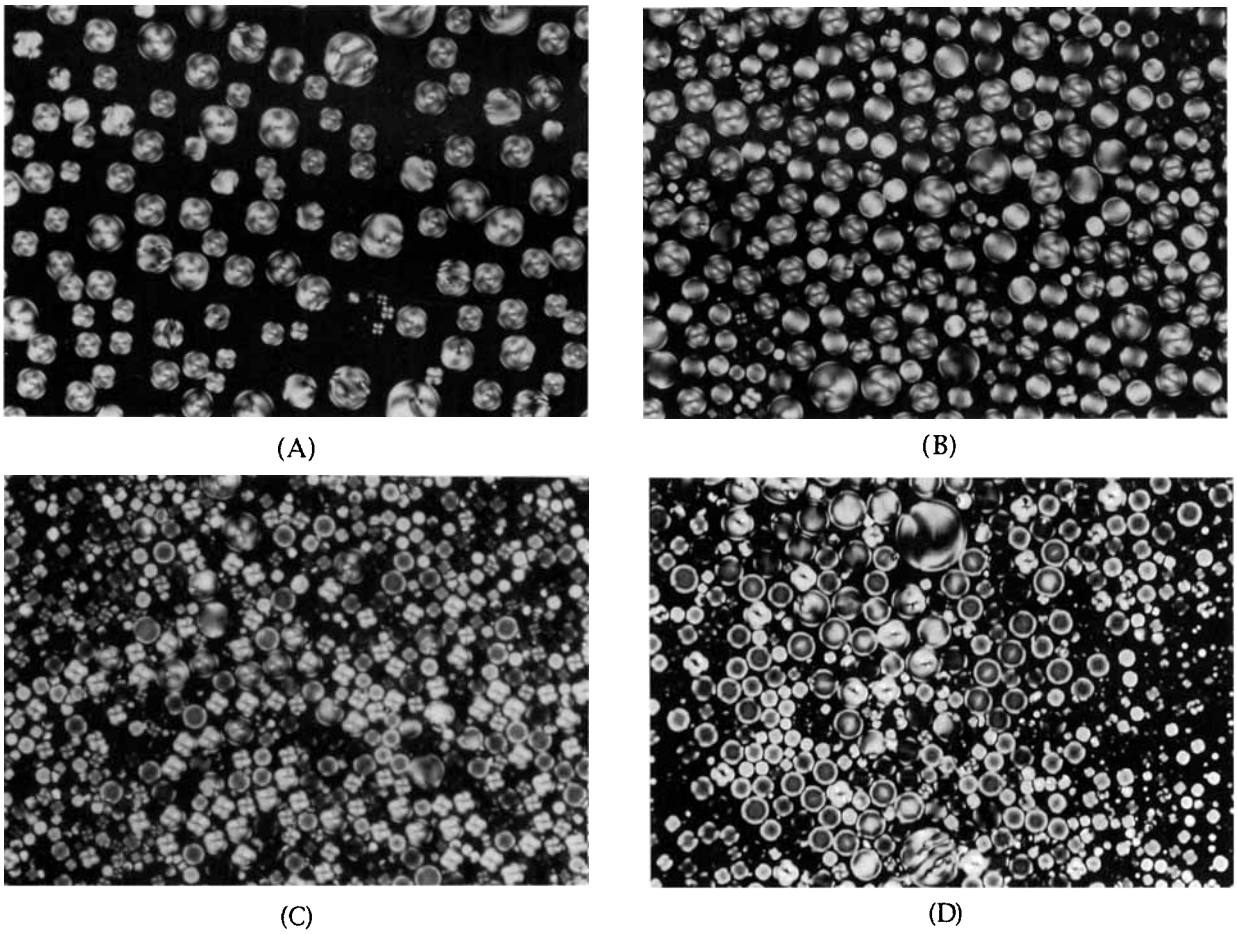

Figure 4 Polarized optical micrographs (600×) of nematic droplets of (PMABD-*co*-POE) polymers: (A) #2, obtained at 140°C; (B) #3, obtained at 136°C; (C) #4, obtained at 133°C; (D) #5, obtained at 133°C.

enthalpy, ΔH_{kn} and ΔH_{ni}, and of the entropy of phase transitions, ΔS_{kn} and ΔS_{ni}. It is found that the thermotropic properties of #1, T_g, T_m, T_i, ΔH_{kn}, ΔH_{ni}, ΔS_{kn}, and ΔS_{ni}, are closed to those reported by Blumstein et al.[9,12,13] As PMABD is chemically incorporated with POE, the thermal transition behaviors change significantly. The copolymers do not exhibit cold crystallization as the PMABD does. Obviously, the crystallizability of PMABD in the copolymers has been improved by introducing flexible PEOD chains. The T_m and T_i decrease, and the mesophase range reduces about 6–16°C. Also, the changes of enthalpy and entropy for both melting and mesophase transitions become a third or a quarter ($n < 17$) those of PMABD. The observations reveal that the flexible PEOD chain profoundly reduces not only the order of conformation of both the crystalline and LC phases but also the intermolecular interaction forces.

Mesophase Texture

In the work, two samples of PMABD with $n = 8$ and 20 were prepared for the study of the chain length effect for the mesophase textures of PMABD. Figure 3 shows the pictures of the polarized optical microscopy for the mesophases of the two PMABDs obtained at 132°C ($n = 8$) and at 145°C ($n = 20$). They appear as typical nematic droplets (NDs) characterizing a single center defect with cross brushes as well as a two surface-point defects boojums. Utilizing the simulated pictures of polarizing microscope texture of nematic droplets with the director configuration reported by Kitzerow[21] and Ondris-Crawford et al.,[22] the NDs are known to comprise the plannar anchoring of the bipolar configuration. The chain length does not change the texture of the mesophase. However, the longer n gives a higher onset temperature of the mesophase.

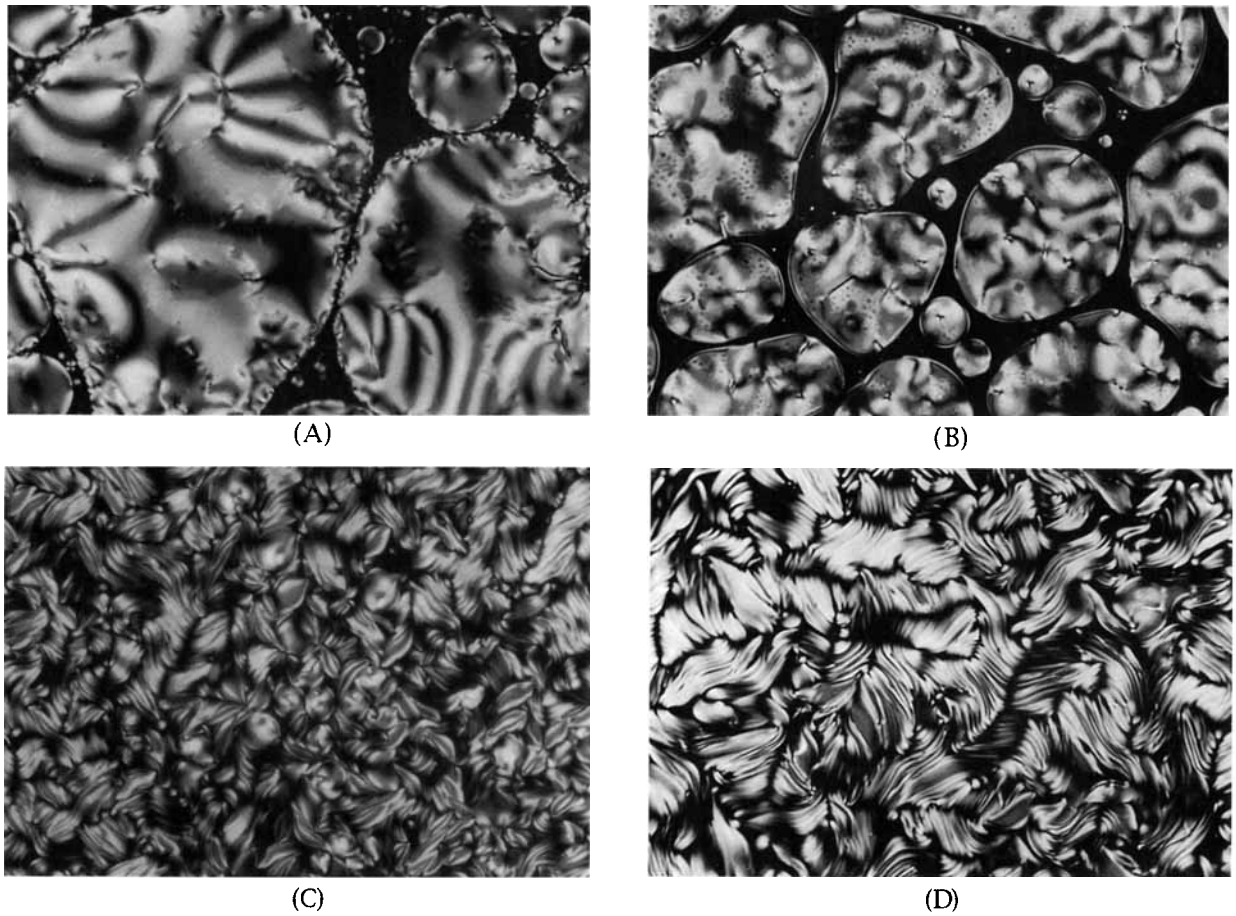

Figure 5 Polarized optical micrographs (600×) of mesophase texture of polymers obtained just before crystallizing: (A) #1, at 129°C; (B) #2, at 120°C; (C) #4, at 118°C; (D) #5, at 117°C.

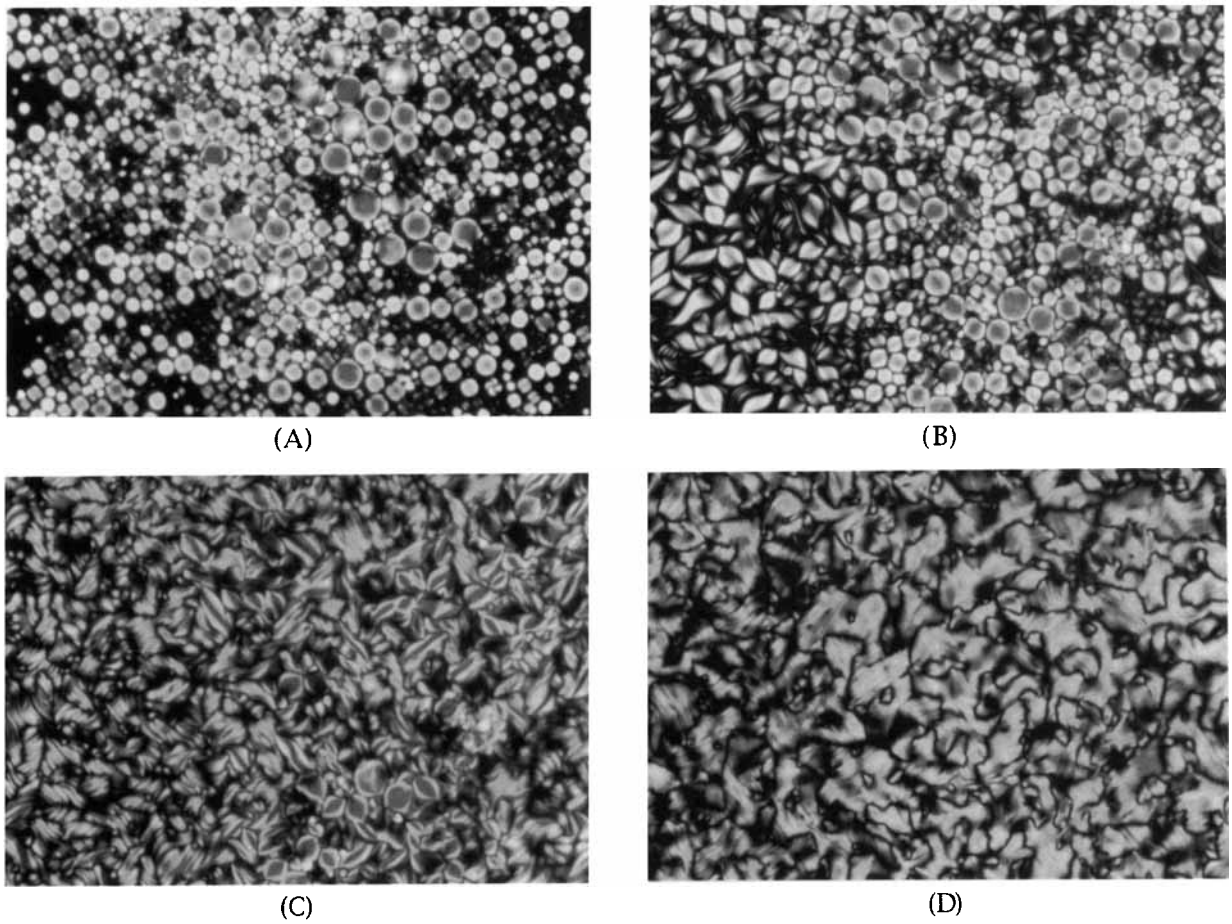

Figure 6 Thermal history of segmented (PMABD-*co*-POE) polymer, #6, observed by polarized optical microscopy (600×) during the cooling process: (A) The texture of nematic droplets obtained at 133°C, the transition states obtained at (B) 130°C and (C) 126°C, and (D) the distorted-stripe texture obtained at 120°C.

Figure 4 shows the structure of NDs obtained by the series of (PMABD-*co*-POE) polymers. The NDs exhibit two patterns: One, denoted as an A-type, looks like a four-blade fan in which there is a small windmill in its center. The other, denoted as a B-type, shows curved brushes connecting two surface-point-defect boojums. These characteristic patterns indicate that the NDs comprise the structure with plannar anchoring of twisted bipolar configuration. Among them, the A-type comprises the polar axes of the director field parallel to observation, whereas the B-type has the polar axes of the director field vertical to observation. The smaller the n the more the B-type. Note that #2 exhibits only the A-type. Conclusively, the effect of incorporation of POE in PMABD on the mesophase texture changes the NDs from a bipolar configuration to a twisted bipolar one, even for #2, which comprises simply two PMABD's (n = 20) and a single PEOD. The larger ratio of PEOD to PMABD makes chains more flexible. Consequently, those copolymers with a smaller n prefer to produce the NDs with the axes of the director field perpendicular to observation. Hence, the flexibility of polymer chains gaining from the PEOD segment is one of the reasons for obtaining the twisted bipolar configuration.

According to de Gennes,[19] the bend elastic constant K_{33} is dominated by the rigidity of the macromolecular chains, whereas the twist constant K_{22} is mainly a function of the interaction between neighboring chains, and the splay constant K_{11} is predicted to increase with the square of the molecular length. From the results aforementioned, the flexible PEOD chain significantly reduces the intermolecular interaction forces between the PMABD chains, thus causing the reduction of K_{22}. Meanwhile, it also makes the molecular chains more flexible and then decreases K_{33}. As suggested by

Williams[22] and Kitzerow,[21] both effects favor the formation of a twisted bipolar configuration, and it is expected to occur even for nonchiral liquid crystals.

Figure 5 illustrates the pictures of polarized optical microscopy for the mesophases of copolymers obtained just before crystallizing. As expected, sample #1 (PMABD) grows a typical nematic Schlieren texture [Fig. 5(A)]. Similar to #1, those A-type NDs of #2 and #3 finally grow to be a Schlieren texture [Fig. 5(B)]. However, as illustrated in Figure 5(C) and (D), #4 and #5 finally obtain the texture of alternative yellow/brown, and/or yellow/blue/red distorted stripes.

Figure 6 illustrates the growing of LC of #6 under the cooling process. It is observed that the NDs subsequently changed to a broad leaflike conformation and then to an elongated and somewhat twisted leaflike one. It finally became a distorted-stripe conformation. Also, the two poles can be clearly observed at both ends of the stripes. Note that the size of NDs is nearly unchanged during the undercooled process. The growths of #4 and #5 are similar. By carefully examining the pictures of #4, #5, and #6, one can easily find that, especially for #4, in addition of the distorted-stripe conformation, there occurs a few of Schlieren-texture domains that were observed in #1–#3. The fraction of it decreases from #4 to #6. The Schlieren-texture conformation is reasonally assumed to be obtained from the A-type NDs, whereas the distorted-stripes conformation is obtained from the B-type NDs. The occurrence of A-type NDs in the copolymers #4–#6 implies that it includes some fraction of the copolymer whose composition is near #3 and/or #2, and they significantly decrease from #4 to #6. Furthermore, it is found that two types of NDs independently grow in the undercooled process. Thereby, the copolymers with a composition corresponding to #3 and/or #2 are incompatible with those of #4 to #6.

From the results aforementioned, the distorted-stripe conformation may arise from the following reasons: As mentioned above, the twisted bipolar configuration of NDs is due to gaining of the chain flexibility owing to the PEOD segment. On the other hand, under the cooling process, those flexible chains easily become somewhat more rigid with decreasing temperature and increase the bend elastic constant K_{33}.[24,25] The effect reduces the bending of the director and aligns the directors toward the axis of the poles. Furthermore, from the characteristics of the DSC thermograms of the copolymers obtained, it may be assumed that several small domains neighboring those LC domains of PMABD profoundly hinder those NDs to join together, owing to incompatibility between both domains of PMABD and PEOD.

CONCLUSIONS

The consequences of alternatively copolymerizing PMABD segments and flexible POE 400 for the mesomorphic behaviors and the thermotropic properties lead to the obtainment of a new PEOD chain linking between PMABD segments as well as the domains of PMABD and PEOD. In addition to lowering both the enthalpy and entropy changes of K/N and N/I transitions, and narrowing the temperature range of the mesophase, the flexible PEOD chains cause the PMABD segment to form a twisted bipolar configuration of nematic droplets. Subsequently, under the cooling process, the effects of the chain flexibility of PEOD and the incompatibility of PMABD and PEOD domains induce a distorted-stripe conformation before crystallizing.

REFERENCES

1. A. Roviello and A. Sirigu, *J. Polym. Sci. Polym. Lett.*, **13,** 455 (1975).
2. A. Roviello and A. Sirigu, *Eur. Polym. J.*, **15,** 61 (1979).
3. K. Iimura, N. Koide, and R. Ohta, *Rep. Prog. Polym. Phys. Jpn.*, **24,** 231 (1981).
4. A. C. Griffin and S. J. Havens, *J. Polym. Sci. Part B Polym. Phys.*, **19,** 1901 (1981).
5. J.-I. Jin, R. W. Lenz, and S. Antoun, *J. Kor. Chem. Soc.*, **26,** 188 (1982).
6. G. Galli, E. Chiellini, C. K. Ober, and R. W. Lenz, *Makromol. Chem.*, **183,** 2693 (1982).
7. V. Pearces, H. Nava, and H. Jonsson, *J. Polym. Sci. Part A Polym. Chem. Ed.*, **25,** 1943 (1987).
8. D. Van Luyen, L. Liebert, and L. Strzelecki, *Eur. Polym. J.*, **16,** 307 (1980).
9. A. Blumstein, *Polym. J.*, **17,** 277 (1985).
10. S. Vilasagar and A. Blumstein, *Mol. Cryst. Liq. Cryst. Lett.*, **56,** 263 (1980).
11. S. Vilasagar and A. Blumstein, *Mol. Cryst. Liq. Cryst. Lett.*, **72,** 1 (1981).
12. A. Blumstein, S. Vilasagar, S. Ponrathnam, and S. B. Clough, *J. Polym. Sci. Part B Polym. Phys.*, **20,** 877 (1982).
13. R. B. Blumstein, E. M. Stickles, M. M. Gauthier, and A. Blumstein, *Macromolecules,* **17,** 177 (1984).
14. V. V. Zuev, G. S. Smirnova, and N. A. Nikonorova, *Makromol. Chem.*, **191,** 2865 (1990).

15. R. W. Lenz and J.-I. Jin, *Macromolecules,* **14,** 1405 (1981).
16. A. K. Rao, R. W. Lenz, and J.-I. Jin, *Br. Polym. J.,* **21,** 473 (1989).
17. G. Q. Chen and R. W. Lenz, *J. Polym. Sci. Part A Polym. Chem. Ed.,* **22,** 3189 (1984).
18. T. Shaffer and V. Pearces, *J. Polym. Sci. Polym. Lett. Ed.,* **23,** 185 (1985).
19. P. G. De Gennes, *Mol. Cryst. Liq. Cryst.,* **34,** 177 (1977).
20. N. J. Leonard and J. W. Curry, *J. Org. Chem.,* **17,** 1071 (1952).
21. H.-S. Kitzerow, *Liq. Cryst.,* **16,** 1 (1994).
22. R. Ondris-Crawford, E. P. Boyko, B. G. Wagner, and J. H. Erdmann, *J. Appl. Phys.,* **69,** 6380 (1991).
23. R. D. Williams, *J. Phys. A Math. Gen.,* **19,** 3211 (1986).
24. H. Kelker, R. Hatz, and C. Schumann, in *Handbook of Liquid Crystals,* Deerfield-Verlag Chemie, Weinheim, 1980, p. 120.
25. S. Chandrasekhar, in *Liquid Crystals,* 2nd ed., Cambridge University Press, New York, 1992, p. 59.

Received July 9, 1994
Accepted September 7, 1994